Science Advances

AAAS

advances.sciencemag.org/cgi/content/full/3/5/e1602680/DC1

Supplementary Materials for

Emergence of topological semimetals in gap closing in semiconductors without inversion symmetry

Shuichi Murakami, Motoaki Hirayama, Ryo Okugawa, Takashi Miyake

Published 12 May 2017, *Sci. Adv.* **3**, e1602680 (2017)
DOI: 10.1126/sciadv.1602680

This PDF file includes:

Supplementary Text

More examples for gap closing with various symmetries

In the main text we gave four examples for closing of the gap, classified by the *k*-group of the **k** point considered: (i) no symmetry, (ii) twofold rotation C_2, (iii) C_2 and $\Theta C'_2$, and (iv) mirror reflection M. Here we give more examples, in order to demonstrate evolution of the band structure as the value of the parameter m changes. As explained in the Methods section in the main text, we consider the Hamiltonian of the form $H(\mathbf{q}, m)=\sum_{i=1}^{3} a_i(\mathbf{q},m)\sigma_i$, where σ_i ($i = x,y,z$) are Pauli matrices, and $\mathbf{q} = \mathbf{k}-\mathbf{k}_0$. We assume $a_i(\mathbf{q}=0, m=m_0)=0$, i = 1,2,3. We also assume that when $m<m_0$ the gap is open.

(v) ΘC_2 symmetry: We consider a **k** point which is invariant only under an operation ΘC_2, where Θ is the time-reversal operation. Let z denote a coordinate along the C_2 axis. The Hamiltonian then satisfies $H(q_x, q_y, q_z, m) = H^*(q_x, q_y,-q_z, m)$. It leads to $a_y = q_z f_y(q_x, q_y, q_z^2, m)$, $a_x = f_x(q_x, q_y, q_z^2, m)$, and $a_z = f_z(q_x, q_y, q_z^2, m)$, where f_i are analytic functions. From these conditions, we can show that the solution at $\mathbf{q}=0$, $m=m_0$ bifurcates into two Weyl nodes, a monopole and an antimonopole on the $q_z=0$ plane, and their trajectories are given by $q_z=0$, $f_x(q_x, q_y, 0, m)=0=f_z(q_x, q_y, 0, m)$. This case is denoted as **1p**, where **p** stands for "planar", meaning that the trajectories of the monopole and the antimonopole are restricted to be within a high-symmetry plane (fig. S1 **A**).

(vi) ΘM symmetry: Suppose the wavevector **k** is invariant under ΘM, where M is a mirror operation. We take the z axis to be perpendicular to the mirror plane. We then obtain $H(q_x, q_y, q_z, m)=H^*(-q_x, -q_y, q_z, m)$, leading to $a_y=q_x f_x(q_x^2, q_y^2, q_z, m)+q_y f_y(q_x^2, q_y^2, q_z, m)$, while a_x and a_z are analytic functions of q_x^2, q_y^2, q_z and m. By retaining the lowest order in the arguments in these functions, one can see that it describes a monopole-antimonopole pair creation and the positions of the monopole and the antimonopole are expressed as $(\tilde{q}_x(m), \tilde{q}_y(m), \tilde{q}_z(m))$ and $(-\tilde{q}_x(m),-\tilde{q}_y(m), \tilde{q}_z(m))$, respectively. They are symmetric with respect to the $q_x=q_y=0$ axis. We call this case **1sp**, where **s** (symmetric) means that the positions of the monopole and the antimonopole are related with each other by symmetry operations (fig. S1 **B**).

(vii) M and $\Theta M'$ symmetries, with mirror planes of M and M' perpendicular to each other: Let us call the mirror planes for M and $\Theta M'$ as xy and xz planes, respectively. There are two representations corresponding to different signs of the eigenvalues of M. Evolution of band structure after closing of the gap is different between (vii-1) the two bands with the same irreducible representations (R_c=R_v), and (vii-2) those with different irreducible representations ($R_c \neq R_v$). For (vii-1), we have $H(q_x, q_y, q_z, m) = H(q_x, q_y, -q_z, m)$, $H(q_x, q_y, q_z, m) = H^*(-q_x, q_y, -q_z, m)$, leading to $a_x = f_x(q_x^2, q_y, q_z^2, m)$, $a_y = q_x f_y(q_x^2, q_y, q_z^2, m)$, $a_z = f_z(q_x^2, q_y, q_z^2, m)$. Therefore, for q_x=0, the gap closes when $f_x(0, q_y, q_z^2, m)=0=f_z(0, q_y, q_z^2, m)$ is satisfied. These two equations determine a curve in the (q_y, q_z, m) space, and this curve is symmetric with respect to $q_z \to -q_z$. This curve passes through the point q_y=0, q_z=0, m=m_0, but does not go into the $m<m_0$ region. Therefore, as we increase m across m_0, the solution at q_y=0=q_z, m=m_0 bifurcates into a pair of Weyl nodes at $\mathbf{q}=(0, \tilde{q}_y(m), \pm\tilde{q}_z(m))$. It is denoted as **1sa** (fig. S1 **C**). For the case (vii-2) $R_c \neq R_v$, because the mirror symmetry persists for all the **k** points within the mirror plane (xy plane), it gives rise to a nodal-line semimetal after closing of the gap, denoted by **1ℓ**.

Classification tables for emergent topological semimetals after closing of the band gap of inversion-asymmetric insulators

In the main text, we have shown that patterns for emergence of Weyl nodes and nodal lines after closing of the gap are uniquely determined by symmetry, i.e. by the space group and by the value of $\mathbf{k}_0$ where the gap closes. Here all the patterns for Weyl nodes and nodal lines for all the 138 space groups are shown in Fig. 4. Notations used in this figure are summarized as follows.

- The numbers in the symbols in e.g. **1s** and **1sp** represent the number of pair of Weyl nodes, except for **1ℓ**, **2ℓ**, **3ℓ**, **4ℓ**, where the number represents a number of nodal lines.
- The symbol **ℓ** means that there is a nodal line where the gap is closed. Such a nodal line always appears as a loop on mirror planes, and only when the valence and the conduction bands have different mirror eigenvalues.
- The symbol **a** (axial) represents that relative directions between the Weyl nodes are fixed to be along certain high-symmetry lines.

- The symbol **p** (planar) represents that relative directions between the Weyl nodes are not confined to be a high-symmetry axis, but confined within a high-symmetry plane.
- The symbol **c** (coplanar) means that all the monopoles and antimonopoles lie on a same high-symmetry plane. This symbol c is used only when there are more than one monopole-antimonopole pairs.
- The symbol **t** (tetrahedral) appears only for a few cases with tetrahedral or cubic symmetries. It means that the 4 monopoles and 4 antimonopoles form 8 vertices of a cube whose center is a high symmetry point, and 4 monopoles form a tetrahedron.
- The symbol **s** (symmetric) means that all the monopoles and antimonopoles are related to each other by symmetry operations. In such cases they are energetically degenerate, and it is possible to locate all the Weyl nodes on the Fermi energy. Otherwise, these monopoles and antimonopoles may not necessarily be at the same energy.

Apart from these patterns in Fig. 4, their combinations can appear, such as **1sa1ℓ** (e.g. at *K* and *H* points in No.**174** and No.**187**), which means that one pair of Weyl nodes and one nodal line are simultaneously created at closing of the gap. In addition, when there are more than one mirror planes at $\mathbf{k}_0$, more than one nodal lines can be created (e.g. **2ℓ**, **3ℓ**, **4ℓ**), and they are on different mirror planes, intersecting each other at $\mathbf{k}_0$.

In the following, we explain how these patterns emerge for various **k** points in 138 space groups without inversion symmetry. Time-reversal symmetry is assumed throughout. All the cases are classified in terms of space groups and values of $\mathbf{k}_0$ where the gap closes. Then, various cases for each **k** point are classified in terms of irreducible representation of the conduction band and that of the valence band, denoted as R_c and R_v, respectively. As explained in the main text, we have to study only the cases with dim R_c=dim R_v=1 because otherwise the gap cannot close $\mathbf{k}_0$. In particular, one can exclude the TRIM as $\mathbf{k}_0$, since there is always Kramers degeneracy at the TRIM, and the gap cannot close. In addition, if a high-symmetry point shares the same *k*-group with a high-symmetry line which includes this point, the gap does not close at the high-symmetry point, because it requires fine-tuning of the Hamiltonian.

In the following tables, we show the high-symmetry points and lines, where the gap can close by changing a single parameter m. It should be noted that in addition to the patterns listed in the following tables, the following two patterns exist, which are common to all the space groups.

- generic **k** without any symmetry: **1** (the case (i) in the main text)
- generic **k** on a mirror plane: **1sa** for $R_c = R_v$ (the case (iv-1)), and **1ℓ**, for $R_c \neq R_v$ (the case (iv-2)). In the former case, the conduction and valence bands have the same signs of mirror eigenvalues, while in the latter, they have the opposite signs.

In tables S1-S5, we show all the patterns for the combinations of R_c and R_v, where the gap can close by changing the parameter m. Cases where the gap cannot close at $\mathbf{k}_0$ are excluded from the tables. We show all the 138 space groups without inversion symmetry. In the tables "point" and "line" refer to the high-symmetry points and the high-symmetry lines, respectively. As noted above, R_c and R_v should be both one-dimensional. The names of the irreducible representations (irreps) follows the notation in Ref. (*36*), such as R_1 and R_2, and so on. For a concise expression in the tables, we use the symbols "ii" and "ij"; "ii" means the case with $R_c=R_v$ and "ij" means the case with $R_c \neq R_v$. When there is only one representation allowed at the **k** point, such symbols are not needed and thus are not shown. For more complicated cases, for example, the entry (3,4) in the tables means (R_3, R_4), representing to two cases (R_c, R_v) = (R_3, R_4), (R_4, R_3).

Furthermore, some lengthy entities are abbreviated in the following way:

[1]=(R_2,R_3)(R_4,R_5); **2ℓ**, (R_2,R_4)(R_3,R_5)(R_2,R_5)(R_3,R_4); **1ℓ**.

[2]=(R_5,R_6)(R_6,R_7)(R_7,R_8)(R_8,R_5); **1sa**, (R_5,R_7)(R_6,R_8); **2sp**.

[3]=(R_2,R_5)(R_3,R_4); **2ℓ**,(R_2,R_3)(R_4,R_5)(R_2,R_4)(R_3,R_5); **1ℓ**.

[4]=(R_5,R_6)(R_6,R_7)(R_7,R_8)(R_8,R_5); **1sa**, (R_5,R_7)(R_6,R_8); **2sa**.

[5]=(R_3,R_4)(R_5,R_6); **2ℓ**, (R_3,R_5)(R_4,R_6); **2sca**, (R_3,R_6)(R_4,R_5); **1ℓ**

[6]=(R_{11},R_8)(R_{10},R_9)(R_7,R_{12}); **1ℓ**, (R_{11},R_7)(R_{10},R_8)(R_7,R_9)(R_8,R_{12})(R_9,R_{11})(R_{12},R_{10}); **1sa**, (R_{11},R_{10})(R_{10},R_7)(R_7,R_8)(R_8,R_9)(R_9,R_{12})(R_{12},R_{11}); **1sa1ℓ**.

[7]=(R_4,R_5)(R_5,R_6)(R_6,R_4); **4st**.

[8]=(R_4,R_7)(R_5,R_6); **4ℓ**, (R_4,R_5)(R_6,R_7); **3ℓ**, (R_4,R_6)(R_5,R_7); **1ℓ**.

Properties of band structure of HfS

Here we briefly explain the band structure of HfS and the reason why it is appropriate as a candidate for a nodal-line semimetal. The crystal structure of HfS is the same as that of tungsten carbide (WC). Its space group is No. **187** ($P\bar{6}m2$) (*38*), and it has several mirror planes, which are necessary for the Weyl nodal lines by mirror symmetry as we discussed. Bands of the Hf 5*d* orbitals are classified into three groups, a'_1, e', and e'', by the crystal field from a trigonal prism of S^{2+} atoms. A narrow gap is formed between the occupied a'_1 band and the unoccupied e' bands. A layered triangle lattice formed by Hf atoms is favorable for displacing the point of the minimum band gap away from the Γ point to the *K* point by interference effects. When the spin-orbit coupling (SOC) is neglected, a Dirac nodal-line exists around the *K* point on the $k_z = 0$ plane.

When the SOC is considered, due to mismatch between threefold rotational symmetry of the trigonal prism and the right angle of electronic clouds of atomic *d* orbitals, wavefunctions become necessarily complex, and a relativistic energy splitting would be partially enhanced. Spin splitting vanishes at the TRIM, while it is prominent at the non-TRIM points such as *K*- and *H*-points. Thus the SOC lifts the degeneracy in the Dirac nodal-line, and the Weyl nodal-line appears instead near the *K* point on the mirror plane $k_z = 0$

Phonon Dispersion of HfS

We check dynamic stability of HfS at ambient pressure and under pressure in the LDA of the DFPT. The phonon dispersion at ambient pressure and at 20 GPa is shown in fig. S2 **A** and **B**, respectively. The structure is at least metastable up to 20 GPa, since there is no imaginary frequency in the phonon dispersion.

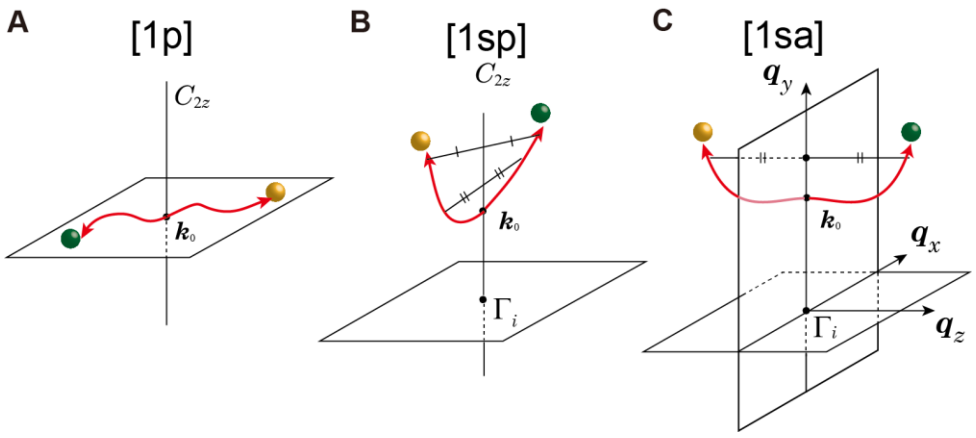

fig. S1. Trajectories of Weyl nodes after a pair creation at k_0 for representative cases. (**A**), (**B**), and (**C**) show the cases (v), (vi), and (vii-1), respectively. Yellow and green spheres denote monopoles and antimonopoles in **k** space, respectively, and they are both Weyl nodes.

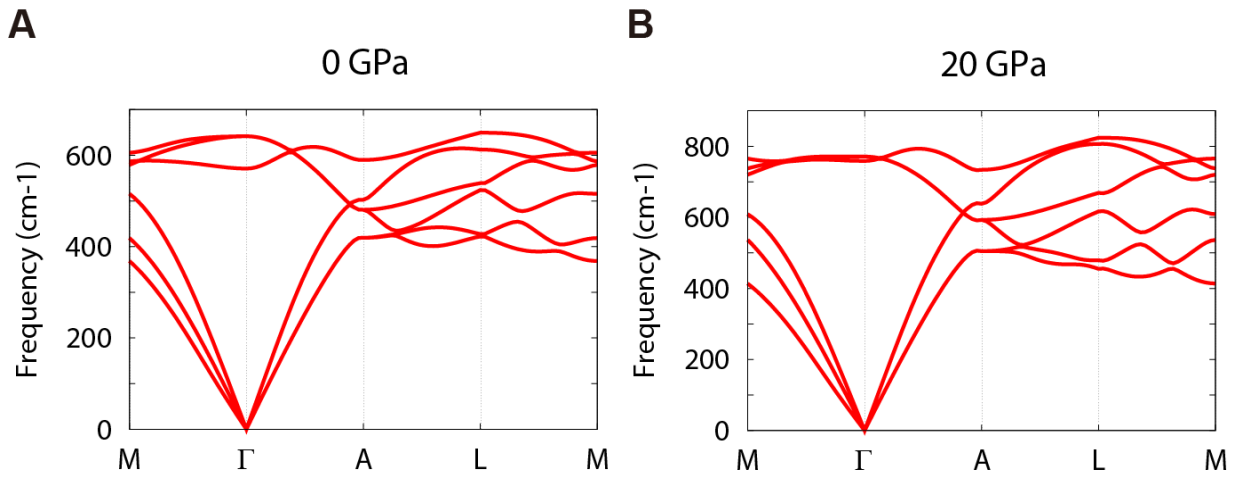

fig. S2. Phonon dispersion of HfS. (**A** and **B**) show the calculated phonon dispersions of HfS at 0 GPa and 20 GPa, respectively.

table S1. Patterns of gap-closing points after parametric gap closing for triclinic and monoclinic space groups.

space group		point	line
1	$P1$		
3	$P2$		ΛVWU:ij;**1a**
4	$P2_1$		ΛVWU:ij;**1a**
5	$C2$		ΛU:ij;**1a**
6	Pm		ΛVWU:**1sp**
7	Pc		ΛW:**1sp**
8	Cm		ΛU:**1sp**
9	Cc		Λ:**1sp**

table S2. Patterns of gap-closing points after parametric gap closing for orthorhombic space groups. We note that in No. **38**, **39**, **40** and **41**, despite the space group symbols use the *A* lattice for orthorhombic base-centered Bravais lattice, we use the *C* lattice with the twofold rotation axis is along *y*, following the notations in Ref. (*36*) (see p. 83 and p. 135 in Ref. (*36*))

space group		point	line
16	*P*222		Δ*DPB*Σ*CEA*Λ*HQG*:ii;**2a**,ij;**1a**
17	$P222_1$		Δ*D*Σ*C*Λ*HQG*:ii;**2a**,ij;**1a**
18	$P2_12_12$		Δ*B*Σ*A*Λ:ii;**2a**,ij;**1a**
19	$P2_12_12_1$		ΔΣΛ:ii;**2a**,ij;**1a**
20	$C222_1$		Λ*H*Σ*Δ*FC*:ii;**2a**,ij;**1a** *D*:ij;**1a**
21	*C*222		Λ*HA*Σ*Δ*BGFEC*:ii;**2a**,ij;**1a** *D*:ij;**1a**
22	*F*222		Λ*GHQ*Σ*CAU*Δ*DBR*:ii;**2a**,ij;**1a**
23	*I*222		Λ*G*Σ*F*Δ*U*:ii;**2a**,ij;**1a** *PDQ*:ij;**1a**
24	$I2_12_12_1$	*W*:ij;**2a**	Λ*G*Σ*F*Δ*U*:ii;**2a**,ij;**1a** *PDQ*:ij;**1a**
25	*Pmm*2		Δ*DPB*Σ*CEA*:ii;**1sa**,ij;**1ℓ**
26	$Pmc2_1$		Δ*D*Σ*C*:ii;**1sa**,ij;**1ℓ**
27	*Pcc*2		Δ*D*Σ*C*:ii;**1sa**,ij;**1ℓ**
28	*Pma*2		Δ*DPB*Σ*A*:ii;**1sa**,ij;**1ℓ** *HQ*:[1]
29	$Pca2_1$		Δ*D*Σ:ii;**1sa**,ij;**1ℓ** *HQ*:[1]
30	*Pnc*2		Δ*D*Σ*E*:ii;**1sa**,ij;**1ℓ** *HQ*:[1]
31	$Pmn2_1$		Δ*D*Σ:ii;**1sa**,ij;**1ℓ** *HQ*:[1]
32	*Pba*2		Δ*B*Σ*A*:ii;**1sa**,ij;**1ℓ** *HG*:[1]
33	$Pna2_1$		ΔΣ:ii;**1sa**,ij;**1ℓ** *HG*:[1]
34	*Pnn*2		Δ*P*Σ*E*:ii;**1sa**,ij;**1ℓ** *HG*:[1]
35	*Cmm*2		*D*:ij;**1a** *A*Σ*Δ*BGFEC*:ii;**1sa**,ij;**1ℓ**
36	$Cmc2_1$		*D*:ij;**1a** Σ*Δ*FC*:ii;**1sa**,ij;**1ℓ**
37	*Ccc*2		*D*:ij;**1a** Σ*Δ*FC*:ii;**1sa**,ij;**1ℓ**
38	*Amm*2		Λ*HA*Σ*EC*:ii;**1sa**,ij;**1ℓ** *D*:**1s*P***
39	*Aem*2		Λ*HA*Σ*EC*:ii;**1sa**,ij;**1ℓ**
40	*Ama*2		Λ*H*Σ*C*:ii;**1sa**,ij;**1ℓ** *D*:**1s*P*** *BG*:[3]
41	*Aea*2		Λ*H*Σ*C*:ii;**1sa**,ij;**1ℓ** *BG*:[3]
42	*Fmm*2		Σ*CAU*Δ*DBR*:ii;**1sa**,ij;**1ℓ**
43	*Fdd*2		Σ*U*Δ*R*:ii;**1sa**,ij;**1ℓ** *GH*:[1]
44	*Imm*2	*W*:ij;**1sa**	*P*:ij;**1a** Σ*F*Δ*U*:ii;**1sa**,ij;**1ℓ** *DQ*:**1s*P***
45	*Iba*2		*P*:ij;**1a** Σ*F*Δ*U*:ii;**1sa**,ij;**1ℓ**
46	*Ima*2		*P*:ij;**1a** Σ*F*Δ*U*:ii;**1sa**,ij;**1ℓ** *Q*:**1s*P***

table S3. Patterns of gap-closing points after parametric gap closing for tetragonal space groups.

space group		point	line
75	$P4$		$\Delta U\Sigma SYT$:**1p** ΛVW:ij;**1a**
76	$P4_1$		$\Delta\Sigma Y$:**1p** ΛVW:ij;**1a**
77	$P4_2$		$\Delta U\Sigma SYT$:**1p** ΛVW:ij;**1a**
78	$P4_3$		$\Delta\Sigma Y$:**1p** ΛVW:ij;**1a**
79	$I4$		ΛVW:ij;**1a** $\Sigma F\Delta UY$:**1p**
80	$I4_1$		ΛVW:ij;**1a** $\Sigma F\Delta UY$:**1p**
81	$P\bar{4}$		$\Delta U\Sigma SYT$:**1p** W:ij;**1a**
82	$I\bar{4}$	P:[2]	W:ij;**1a** $\Sigma F\Delta UY$:**1p**
89	$P422$		$\Delta U\Sigma SYTW$:ii;**2a**,ij;**1a** ΛV:ii;**4a**,ij;**1a**
90	$P42_12$		$\Delta U\Sigma S$:ii;**2a**,ij;**1a** Λ:ii;**4a**,ij;**1a**
91	$P4_122$		$\Delta\Sigma YW$:ii;**2a**,ij;**1a** ΛV:ii;**4a**,ij;**1a**
92	$P4_12_12$		$\Delta\Sigma$:ii;**2a**,ij;**1a** Λ:ii;**4a**,ij;**1a**
93	$P4_222$		$\Delta U\Sigma SYTW$:ii;**2a**,ij;**1a** ΛV:ii;**4a**,ij;**1a**
94	$P4_22_12$		$\Delta U\Sigma S$:ii;**2a**,ij;**1a** Λ:ii;**4a**,ij;**1a**
95	$P4_322$		$\Delta\Sigma YW$:ii;**2a**,ij;**1a** ΛV:ii;**4a**,ij;**1a**
96	$P4_32_12$		$\Delta\Sigma$:ii;**2a**,ij;**1a** Λ:ii;**4a**,ij;**1a**
97	$I422$		ΛV:ii;**4a**,ij;**1a** $W\Sigma F\Delta UY$:ii;**2a**,ij;**1a** Q:ij;**1a**
98	$I4_122$	P:(2,3);**4a**	ΛV:ii;**4a**,ij;**1a** $W\Sigma F\Delta UY$:ii;**2a**,ij;**1a** Q:ij;**1a**
99	$P4mm$		$\Delta U\Sigma SYT$:ii;**1sa**,ij;**1ℓ**
100	$P4bm$		$\Delta U\Sigma S$:ii;**1sa**,ij;**1ℓ** W:[3]
101	$P4_2cm$		$\Delta\Sigma SY$:ii;**1sa**,ij;**1ℓ**
102	$P4_2nm$		$\Delta\Sigma ST$:ii;**1sa**,ij;**1ℓ** W:[3]
103	$P4cc$		$\Delta\Sigma Y$:ii;**1sa**,ij;**1ℓ**
104	$P4nc$		$\Delta\Sigma T$:ii;**1sa**,ij;**1ℓ** W:[3]
105	$P4_2mc$		$\Delta U\Sigma YT$:ii;**1sa**,ij;**1ℓ**
106	$P4_2bc$		$\Delta U\Sigma$:ii;**1sa**,ij;**1ℓ** W:[3]
107	$I4mm$		$\Sigma F\Delta UY$:ii;**1sa**,ij;**1ℓ** Q:1sp
108	$I4cm$		$\Sigma F\Delta UY$:ii;**1sa**,ij;**1ℓ**
109	$I4_1md$	P:(13,14);**2ℓ**	W:[3] $\Sigma F\Delta$:ii;**1sa**,ij;**1ℓ** Q:1sp
110	$I4_1cd$		W:[3] $\Sigma F\Delta$:ii;**1sa**,ij;**1ℓ**
111	$P\bar{4}2m$		$\Delta UYTW$:ii;**2a**,ij;**1a** ΣS:ii;**1sa**,ij;**1ℓ**
112	$P\bar{4}2c$		$\Delta UYTW$:ii;**2a**,ij;**1a** Σ:ii;**1sa**,ij;**1ℓ**
113	$P\bar{4}2_1m$		ΔU:ii;**2a**,ij;**1a** ΣS:ii;**1sa**,ij;**1ℓ**
114	$P\bar{4}2_1c$		ΔU:ii;**2a**,ij;**1a** Σ:ii;**1sa**,ij;**1ℓ**
115	$P\bar{4}m2$		ΔUYT:ii;**1sa**,ij;**1ℓ** ΣS:ii;**2a**,ij;**1a**
116	$P\bar{4}c2$		ΔY:ii;**1sa**,ij;**1ℓ** ΣS:ii;**2a**,ij;**1a**
117	$P\bar{4}b2$		ΔU:ii;**1sa**,ij;**1ℓ** ΣS:ii;**2a**,ij;**1a** W:[3]
118	$P\bar{4}n2$		ΔT:ii;**1sa**,ij;**1ℓ** ΣS:ii;**2a**,ij;**1a** W:[3]
119	$I\bar{4}m2$	P:[4]	$W\Delta UY$:ii;**2a**,ij;**1a** ΣF:ii;**1sa**,ij;**1ℓ** Q:1sp
120	$I\bar{4}c2$		$W\Delta UY$:ii;**2a**,ij;**1a** ΣF:ii;**1sa**,ij;**1ℓ**
121	$I\bar{4}2m$		ΣF:ii;**2a**,ij;**1a** Q:ij;**1a** ΔUY:ii;**1sa**,ij;**1ℓ**
122	$I\bar{4}2d$	P:[5]	W:[3] ΣF:ii;**2a**,ij;**1a** Δ:ii;**1sa**,ij;**1ℓ** Q:ij;**1a**

table S4. Patterns of gap-closing points after parametric gap closing for trigonal and hexagonal space groups.

space group		point	Line
143	*P*3		Δ*P*:ij;**1a**
144	$P3_1$		Δ*P*:ij;**1a**
145	$P3_2$		Δ*P*:ij;**1a**
146	*R*3		Λ*P*:ij;**1a**
149	*P*312		Δ*P*:ii;**3a**,ij;**1a** *UTST*'*S*':**1p** Σ*R*:ij;**1a**
150	*P*321	*KH*:(3,4);**3ca**	Δ:ii;**3a**,ij;**1a** *U*Σ*R*:**1p** *PTST*'*S*':ij;**1a**
151	$P3_112$		Δ*P*:ii;**3a**,ij;**1a** *UTST*'*S*':**1p** Σ*R*:ij;**1a**
152	$P3_121$	*KH*:(3,4);**3ca**	Δ:ii;**3a**,ij;**1a** *U*Σ*R*:**1p** *PTST*'*S*':ij;**1a**
153	$P3_212$		Δ*P*:ii;**3a**,ij;**1a** *UTST*'*S*':**1p** Σ*R*:ij;**1a**
154	$P3_221$	*KH*:(3,4);**3ca**	Δ:ii;**3a**,ij;**1a** *U*Σ*R*:**1p** *PTST*'*S*':ij;**1a**
155	*R*32		Λ*P*:ij;**3a**,ij;**1a** *B*Σ*QY*:ij;**1a**
156	*P*3*m*1	*KH*:ij;**1a**	Δ:(3,4);**3ℓ** *U*Σ*R*:ij;**1ℓ** *P*:ij;**1a** *TST*'*S*':**1sp**
157	*P*31*m*		Δ*P*:(3,4);**3ℓ** *UTST*'*S*':ij;**1ℓ** Σ*R*:**1sp**
158	*P*3*c*1	*K*:ij;**1a**	Δ:(3,4);**3ℓ** *P*:ij;**1a** *U*Σ*R*:ij;**1ℓ** *TT*':**1sp**
159	*P*31*c*		Δ*P*:(3,4);**3ℓ** *UTST*'*S*':ij;**1ℓ** Σ:**1sp**
160	*R*3*m*		Λ*P*:(3,4);**3ℓ** *B*Σ*QY*:**1sp**
161	*R*3*c*		Λ*P*:(3,4);**3ℓ** Σ*Q*:**1sp**
168	*P*6		Δ*UP*:ij;**1a** *TST*'*S*'Σ*R*:**1p**
169	$P6_1$		Δ*UP*:ij;**1a** *TT*'Σ:**1p**
170	$P6_5$		Δ*UP*:ij;**1a** *TT*'Σ:**1p**
171	$P6_2$		Δ*UP*:ij;**1a** *TST*'*S*'Σ*R*:**1p**
172	$P6_4$		Δ*UP*:ij;**1a** *TST*'*S*'Σ*R*:**1p**
173	$P6_3$		Δ*UP*:ij;**1a** *TT*'Σ;**1p**
174	$P\bar{6}$	*KH*:[6]	Δ:(4,4):**3scp** *U*:**1sp** *P*:ij;**1a** *TST*'*S*'Σ*R*:ij;**1ℓ**
177	*P*622	*KH*:(3,4);**3ca**	Δ:ii;6a,ij;**1a** *UTST*'*S*'Σ*R*:ii;**2a**,ij;**1a** *P*:ii;**3a**,ij;**1a**
178	$P6_122$	*K*:(3,4);**3ca**	Δ:ii;6a,ij;**1a** *UTT*'Σ:ii;**2a**,ij;**1a** *P*:ii;**3a**,ij;**1a**
179	$P6_522$	*K*:(3,4);**3ca**	Δ:ii;6a,ij;**1a** *UTT*'Σ:ii;**2a**,ij;**1a** *P*:ii;**3a**,ij;**1a**
180	$P6_222$	*KH*:(3,4);**3ca**	Δ:ii;6a,ij;**1a** *UTST*'*S*'Σ*R*:ii;**2a**,ij;**1a** *P*:ii;**3a**,ij;**1a**
181	$P6_422$	*KH*:(3,4);**3ca**	Δ:ii;6a,ij;**1a** *UTST*'*S*'Σ*R*:ii;**2a**,ij;**1a** *P*:ii;**3a**,ij;**1a**
182	$P6_322$	*K*:(3,4);**3ca**	Δ:ii;6a,ij;**1a** *UTT*'Σ:ii;**2a**,ij;**1a** *P*:ii;**3a**,ij;**1a**
183	*P*6*mm*	*KH*:(3,4);**3ℓ**	*P*:(3,4);**3ℓ** *TST*'*S*'Σ*R*:ii;**1sa**,ij;**1ℓ**
184	*P*6*cc*	*K*:(3,4);**3ℓ**	*P*:(3,4);**3ℓ** *TT*'Σ:ii;**1sa**,ij;**1ℓ**
185	$P6_3cm$	*K*:(3,4);**3ℓ**	*P*:(3,4);**3ℓ** *TT*'Σ:ii;**1sa**,ij;**1ℓ**
186	$P6_3mc$	*K*:(3,4);**3ℓ**	*P*:(3,4);**3ℓ** *TT*'Σ:ii;**1sa**,ij;**1ℓ**
187	$P\bar{6}m2$	*KH*:[6]	Δ:(3,4);**3ℓ**, (3,3)(4,4);**3sca** *UTST*'*S*':ii;**1sa**,ij;**1ℓ** *P*:ii;**3a**,ij;**1a**
188	$P\bar{6}c2$	*K*:[6]	Δ:(3,4);**3ℓ**, (3,3)(4,4);**3sca** *UTT*':ii;**1sa**,ij;**1ℓ** *P*:ii;**3a**,ij;**1a** *R*:[1]
189	$P\bar{6}2m$		Δ:(3,4);**3ℓ**, (3,3)(4,4);**3sca** *U*Σ*R*:ii;**1sa**,ij;**1ℓ** *P*:(3,4);**3ℓ**
190	$P\bar{6}2c$	*H*:[8]	Δ:(3,4);**3ℓ**, (3,3)(4,4);**3sca** *U*Σ:ii;**1sa**,ij;**1ℓ** *P*:(3,4);**3ℓ** *SS*':[1]

table S5. Patterns of gap-closing points after parametric gap closing for cubic space groups.

space group		point	Line
195	$P23$		ΔZT:ii;**2a**,ij;**1a** ΣS:**1p** Λ:ij;**1a**
196	$F23$	*W*:ij;**1a**	ΔZ:ii;**2a**,ij;**1a** Λ:ij;**1a** ΣS:**1p**
197	$I23$		ΣG:**1p** Δ:ii;**2a**,ij;**1a** ΛDF:ij;**1a**
198	$P2_13$		Δ:ii;**2a**,ij;**1a** Σ:**1p** Λ:ij;**1a**
199	$I2_13$	*P*:[7]	ΣG:**1p** Δ:ii;**2a**,ij;**1a** ΛDF:ij;**1a**
207	$P432$		ΔT:ii;**4a**,ij;**1a** ΣSZ:ii;**2a**,ij;**1a** Λ:ii;**3a**,ij;**1a**
208	$P4_232$		ΔT:ii;**4a**,ij;**1a** ΣSZ:ii;**2a**,ij;**1a** Λ:ii;**3a**,ij;**1a**
209	$F432$		Δ:ii;**4a**,ij;**1a**Λ:ii;**3a**,ij;**1a** ΣSZ:ii;**2a**,ij;**1a** *Q*:ij;**1a**
210	$F4_132$	*W*:(2,4);**4a**	Δ:ii;**4a**,ij;**1a**Λ:ii;**3a**,ij;**1a** ΣSZ:ii;**2a**,ij;**1a** *Q*:ij;**1a**
211	$I432$		ΣDG:ii;**2a**,ij;**1a** Δ:ii;**4a**,ij;**1a** ΛF:ii;**3a**,ij;**1a**
212	$P4_332$		Δ:ii;**4a**,ij;**1a** Σ:ii;**2a**,ij;**1a** Λ:ii;**3a**,ij;**1a**
213	$P4_132$		Δ:ii;**4a**,ij;**1a** Σ:ii;**2a**,ij;**1a** Λ:ii;**3a**,ij;**1a**
214	$I4_132$	*P*:[7]	ΣDG:ii;**2a**,ij;**1a** Δ:ii;**4a**,ij;**1a** ΛF:ii;**3a**,ij;**1a**
215	$P\bar{4}3m$		ΣS:ii;**1sa**,ij;**1ℓ** Λ:(3,4);**3ℓ** *Z*:ii;**2a**,ij;**1a**
216	$F\bar{4}3m$	*W*:[4]	Λ:(3,4);**3ℓ** ΣS:ii;**1sa**,ij;**1ℓ** *Z*:ii;**2a**,ij;**1a** *Q*:**1sp**
217	$I\bar{4}3m$		ΣG:ii;**1sa**,ij;**1ℓ** Λ(3,4);**3ℓ**
218	$P\bar{4}3n$		Σ:ii;**1sa**,ij;**1ℓ** Λ:(3,4);**3ℓ** *Z*:ii;**2a**,ij;**1a**
219	$F\bar{4}3c$		Λ:(3,4);**3ℓ** ΣS:ii;**1sp**,ij;**1ℓ** *Z*:ii;**2a**,ij;**1a**
220	$I\bar{4}3d$	*P*:(17,18);**6ℓ**	Σ:ii;**1sa**,ij;**1ℓ** Λ:(3,4);**3ℓ** *D*:[1] *F*:(9,10);**3ℓ**